Incremental L1-Norm Linear Discriminant Analysis for Indoor Human Activity Classification

Sivan Zlotnikov,[†] Panos P. Markopoulos,[‡] and Fauzia Ahmad[†]

[‡]Dept. of Electrical and Computer Engineering, Temple University, Philadelphia, PA 19122 [‡]Dept. of Electrical and Microelectronic Engineering, Rochester Institute of Technology, Rochester, NY 14623

Abstract—In this paper, we present an incremental version of L1-norm Linear Discriminant Analysis (L1-LDA) for radarbased indoor human activity classification. Incremental L1-LDA enables refinement of the discriminant basis as more training samples become available during operation. At the same time, it permits adaptation to the specific activity patterns of the human subject of interest, different than the ones on which the original discriminant basis was trained. The incremental version retains the robustness of L1-LDA to outliers among the training data. Using Doppler signatures of various indoor human activities, we demonstrate that the proposed method exhibits enhanced performance over the incremental counterpart of standard linear discriminant analysis when the training data are corrupted and similar performance under nominal training data.

I. Introduction

Monitoring of indoor human activity is of increasing research and development interest for a variety of civilian applications, including home security, remote patient monitoring, and elderly assisted living. Due to its insensitivity to lighting conditions and robustness against visual obstructions, radar is gaining impetus among various contact-less modalities being considered for human activity monitoring [1]–[9].

Radar-based indoor motion classification methods predominantly employ discriminant features extracted from micro-Doppler signatures associated with human activities. A majority of the work has focused on features that are extracted in an automated fashion by optimization of some numerical criterion. Examples of such feature-extraction methods include Principal Component Analysis (PCA) and its variants, and Linear Discriminant Analysis (LDA) and its variants [5], [10]–[13]. Deep learning techniques have also been employed for human activity recognition, but they impose a much higher computational load and require large amounts of training data [4], [6], [14].

Recent work has revealed that linear discriminant subspaces, obtained using LDA, provide superior motion recognition performance over principal components (PCs) and L1-PCs of micro-Doppler signatures [13]. However, LDA is known to be sensitive to the presence of irregular points among the training data. This sensitivity arises due to the squared emphasis on the contribution of each training point in the LDA optimization metric. Strong resistance against irregular training has been obtained though the L1-norm variant of LDA, called L1-LDA, which places a linear emphasis on each data point [15], [16]. It is noted that irregularities in the training data

can arise in human motion monitoring applications due to a variety of reasons, such as mislabeling, radar malfunctions, and intermittent/unexpected non-focal motion interference.

Motivated by the robustness of L1-LDA, we propose an incremental L1-LDA method for indoor human activity recognition. The incremental nature of the proposed method offers two advantages over L1-LDA. First, it provides performance enhancements under small training data conditions by incorporating new training data as it becomes available over the course of system operation. Second, it enables adaptation of activity-class descriptions based on the activity patterns of the specific individual being monitored. We evaluate the performance of the proposed method using experimental data analysis in which outlier-corruption is introduced by mislabeling a few micro-Doppler signatures. We demonstrate that the incremental scheme provides higher classification accuracy as more and more data become available. We also show that incremental L1-LDA outperforms its incremental standard LDA counterpart for corrupted data, while providing comparable performance under nominal data.

The remainder of the paper is organized as follows. In Section II, we describe the radar signal model and the proposed incremental L1-LDA method for human activity classification. Experimental results comparing and contrasting the performance of the proposed method with incremental standard LDA are presented in Section III. Conclusions are provided in Section IV.

II. PROPOSED L1-NORM LDA-BASED CLASSIFICATION

A. Signal Model

Considering a continuous-wave (CW) radar, the baseband return corresponding to a moving point target is expressed as

$$s(t) = a(t)e^{-j\theta(t)} \tag{1}$$

where a(t) and $\theta(t)$ are the respective amplitude and phase of s(t). The derivative of $\theta(t)$ provides the associated Doppler frequency. In contrast, a human subject undergoing an activity can be considered as a collection of moving point targets, with its Doppler signature derived as the superposition of individual point-target Doppler frequencies. As Doppler frequencies associated with human activities are typically time-varying, time-frequency (TF) processing is employed to extract the instantaneous frequency signatures characterizing the human

motions [17]–[19]. Short-Time Fourier Transform (STFT) is the most common TF distribution, and is defined as

$$S(t,f) = \int s(t-\tau)w(\tau)e^{-j2\pi f\tau}d\tau, \qquad (2)$$

where the window function $w(\tau)$ determines the trade-off between time and frequency resolutions. In this paper, we use the *spectrogram*, which is the squared magnitude of the STFT.

B. Incremental L1-Norm LDA

We consider K motion classes and assume initial availability of $N_{\mathrm{tr},k}$ training Doppler signatures from class $k \in \{1,2,\ldots,K\}$. The nth training signature for the kth class is obtained by sampling the corresponding spectrogram in N_t time bins and N_f frequency bins, followed by vectorizing the resulting signature matrix, $\mathbf{S}_{k,n} \in \mathbb{R}^{N_t \times N_f}$. That is,

$$\mathbf{s}_{k,n} = \text{vec}(\mathbf{S}_{k,n}) \in \mathbb{R}^{D \times N_{\text{tr},k}}$$
 (3

where $D=N_tN_f$ and $\mathrm{vec}(\cdot)$ returns the column-wise vectorization of its matrix argument. The motion classifier organizes the $N_{\mathrm{tr},k}$ signatures from the kth class in the training matrix

$$\mathbf{S}_k = [\mathbf{s}_{k,1}, \mathbf{s}_{k,2}, \dots, \mathbf{s}_{k,N_{\text{tr},k}}] \in \mathbb{R}^{D \times N_{\text{tr},k}}, \tag{4}$$

and then zero-centers S_k to obtain

$$\mathbf{S}_k^{(zc)} = \mathbf{S}_k - \mathbf{m}_k \mathbf{1}_{N_{\text{tr},k}}^{\top} \tag{5}$$

where

$$\mathbf{m}_k = \frac{1}{N_{\text{tr.}k}} \mathbf{S}_k \mathbf{1}_{N_{\text{tr.}k}} \tag{6}$$

is the mean of the kth class, $\mathbf{1}_{N_{tr,k}}$ denotes the all-ones vector of length $N_{tr,k}$, and ' \top ' denotes matrix transpose. The linear discriminative L1-basis, \mathbf{U}_{L1} , spanning a d-dimensional subspace with d < D, is obtained by solving the optimization problem [16]

$$\mathbf{U}_{L1} = \underset{\mathbf{U} \in \mathbb{R}^{D \times d}}{\operatorname{argmax}} F_{L1}(\mathbf{U}) \tag{7}$$

where

$$F_{L1}(\mathbf{U}) = \frac{\|\mathbf{U}^{\top} \mathbf{A}_b\|_1}{\|\mathbf{U}^{\top} \mathbf{A}_w\|_1},$$

$$\mathbf{A}_b = [(\mathbf{m} - \mathbf{m}_1) N_{\mathsf{tr},1}, \dots, (\mathbf{m} - \mathbf{m}_K) N_{\mathsf{tr},K}],$$
$$\mathbf{A}_w = [\mathbf{S}_1^{(zc)}, \dots, \mathbf{S}_K^{(zc)}],$$

and

$$\mathbf{m} = \frac{1}{N} \sum_{k=1}^{K} N_{\text{tr},k} \mathbf{m}_k.$$

We solve (7) by using the algorithm of [16], reproduced in Fig. 1 for completeness where $P(\mathbf{A}) = \mathbf{A}(\mathbf{A}^{\top}\mathbf{A})^{-1/2}$ for any matrix \mathbf{A} . In the sequel, for brevity, we summarize the aforementioned operations for determiniung the L1 discriminative subspace in the functional form $\mathbf{U}_{L1} = \text{L1-LDA}(\{\mathbf{S}_k\}_{k=1}^K, \mathbf{U}^{(0)}, \beta)$, where $\mathbf{U}^{(0)}$ is a feasible initialization and $\beta \in [0, 1]$.

L1-LDA Basis Calculation

Input: A_b and A_w , initial $U, \beta \in [0, 1]$

1: for n = 1, 2, ... (until convergence) 2: $\mathbf{U}_{old} \leftarrow \mathbf{U}$ 3: $\mathbf{G} \leftarrow \mathbf{A}_b \operatorname{sgn}(\mathbf{A}_b^{\top} \mathbf{U}_{old}) - F(\mathbf{U}_{old}) \mathbf{A}_w \operatorname{sgn}(\mathbf{A}_w^{\top} \mathbf{U}_{old})$ 4: $m \leftarrow 1$ 5: $\mathbf{U} \leftarrow P(\mathbf{U}_{old} + \beta^m \mathbf{G})$ 6: If $F_{L1}(\mathbf{U}) < F_{L1}(\mathbf{U}_{old})$, set $m \leftarrow m + 1$ and repeat step (5) Output: $\mathbf{U}_{L1} \leftarrow \mathbf{U}$

Fig. 1: L1-LDA algorithm [16] for approximately solving (7).

Let $\mathbf{U}_{\mathrm{L}1}^{(0)}$ be the solution of (7) corresponding to the initial training data. As more data become available during operation of the system, we can update the bases as follows. At the nth update index, $n=1,2,\ldots$, we consider that an additional training point from one or more classes becomes available. Accordingly, we define the updated training data matrices $\{\mathbf{S}_k^{(n)}\}_{k=1}^K$. That is, if a single additional training point s from the kth class becomes available, we update the training data as $\mathbf{S}_k^{(n)} = [\mathbf{S}_k^{(n-1)}, \mathbf{s}]$. On the other hand, we can perform a batch update by appending m_1 available class k signatures, $\mathbf{S}_{\mathrm{batch},k} \in \mathbb{R}^{D \times m_1}$, as $\mathbf{S}_k^{(n)} = [\mathbf{S}_k^{(n-1)}, \mathbf{S}_{\mathrm{batch},k}]$ Then, the L1-LDA basis can be updated to the new training data as

$$\mathbf{U}_{\text{update}} = \text{L1-LDA}(\{\mathbf{S}_{k}^{(n)}\}_{k=1}^{K}, \mathbf{U}_{\text{L1}}^{(n-1)}, \beta), \tag{8}$$

$$\mathbf{U}_{\mathrm{L}1}^{(n)} = \Omega\left((1-\gamma)\mathbf{U}_{\mathrm{L}1}^{(n-1)} + \gamma\mathbf{U}_{\mathrm{update}}\right) \tag{9}$$

where $\Omega(\cdot)$ returns an orthonormal basis for its tall matrix argument and γ is the adaptation regularizer that takes values in [0,1]. In practice, the size of $\mathbf{S}_k^{(n)}$ cannot be increased indefinitely. Therefore, when the highest permissible number of columns for $\mathbf{S}_k^{(n)}$ is reached, the oldest measurements in $\mathbf{S}_k^{(n)}$ are dropped to release space for the newly collected training points.

C. Classification

When a discriminative basis \mathbf{U}_{L1} is trained, the classifier projects a test sample, \mathbf{s}_t , on \mathbf{U}_{L1} and then classifies it by means of any standard classification algorithm. In this paper, we employ the nearest-centroid classification [13], wherein the classifier decides that \mathbf{s}_t belongs to the lth activity class if l minimizes

$$d_{\mathrm{L1}}(\mathbf{s}_t; l) = \|\mathbf{U}_{\mathrm{L1}}^{\top}(\mathbf{s}_t - \mathbf{m}_l)\|_2. \tag{10}$$

III. EXPERIMENTAL RESULTS

We consider four different activities, namely, falling, bending, sitting, and walking. Using a 6 GHz CW radar, we collected 30 Doppler signatures from each class in a laboratory environment. Five different human subjects participated in the experiments, who repeated each activity 6 times. All activities were performed along the line-of-sight of the radar, with falling, sitting, and bending at a distance of 2.75 m, while the walking motion was carried out between 1.5 m to 4.5 m away

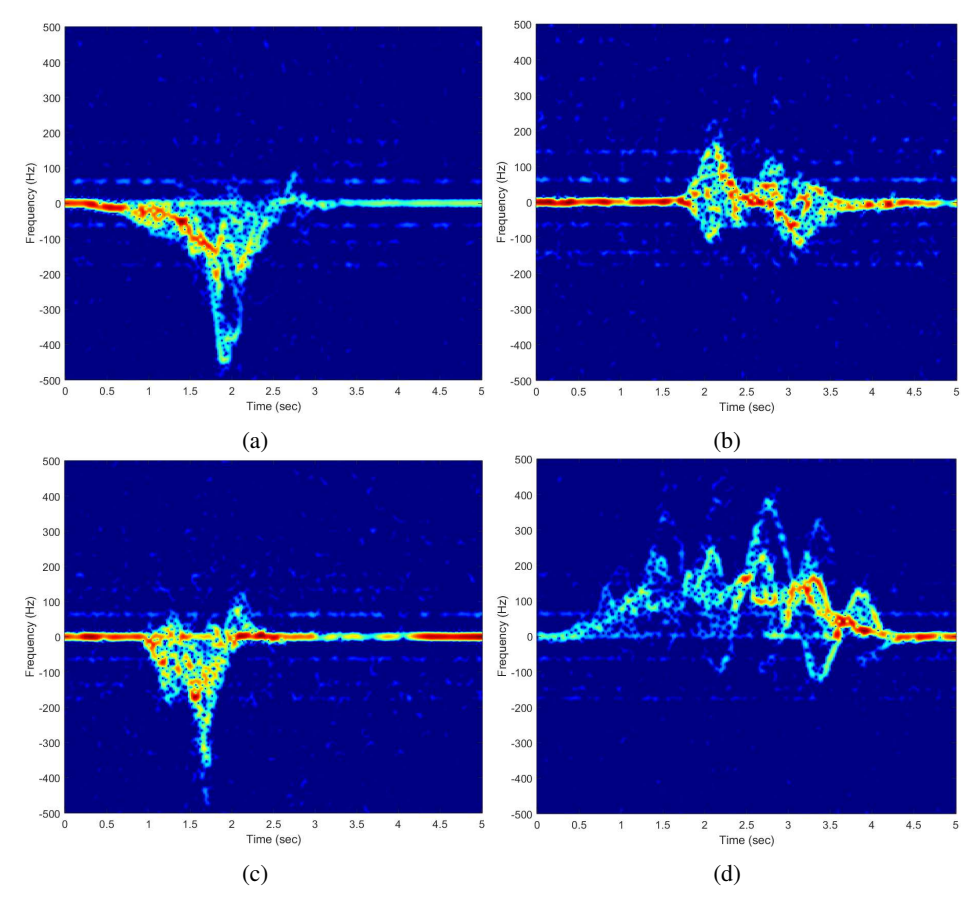


Fig. 2: Doppler signatures corresponding to (a) Falling, (b) Bending to pick up an object, (c) Sitting, and (d) Walking.

from the radar. The feed point of the antenna was positioned 1 m above the floor and a sampling rate of 1 kHz was used for data collection. One Doppler signature corresponding to each of the four activities is illustrated in Fig. 2.

We perform four-way classification, with the classes being fall, bend, sit, and walk. The experimental dataset comprising 30 signatures from each class is augmented by means of the SMOTE method [20], resulting in a total of N=40 measurements per class. The subspace dimensionality is set to d=3. We apply the proposed incremental L1-LDA based classifier and compare its performance with a similar incremental implementation of standard LDA. We initially train $U^{(0)}$ on $N_{tr} = 6$ data points from each of the four activity classes. Then, we update the solution on 34 more measurements from each class in two different manners. We first emulate the single-sample increment scenario, followed by a batchincrement version, with a batch size of three samples. Further, we assume that the maximum allowable number of columns for $\mathbf{S}_{k}^{(n)}$ is 20. As such, beyond 20 measurements, we drop an appropriate number of oldest measurements in $\mathbf{S}_{k}^{(n)}$ to make space for the newly collected training points. The performance is evaluated over 100 independent selections of training and testing data. We asses the classification performance in terms of mean accuracy rate, which is defined as the number of correct classifications versus number of evaluation signatures classified. In Fig. 3, we plot the mean accuracy rate of single-sample incremental versions of L1-LDA and standard LDA for $\gamma=0.9$, versus the increment index. The mean accuracy rate for the batch-incremental versions are provided in Fig. 4. From both Figs. 3 and 4, we observe that, as expected, the performance of both methods increases as more training points become available, with LDA exhibiting slightly higher accuracy than L1-LDA.

Next, we repeat this experiment in the presence of outliers among the training samples. For the single-sample increment case, we consider mislabeling of two out of the four new samples that arrive at increment index 14 and at again increment index 22. More specifically, we consider that one falling sample is mislabeled as sitting and vice versa. The corresponding results are also provided in Fig. 3. We note that the standard LDA is significantly affected by these mislabelings, as evident from the drop in its performance at both indices where the mislabelings were introduced. Moreover, we note that the performance again improved at index 34, since at this point, the mislabeled samples introduced at index 14 were removed from $\mathbf{S}_{k}^{(n)}$ whose maximum capacity is set as 20 samples. On the other hand, the proposed L1-LDA exhibits much less sensitivity to the mislabelings. Furthermore, since the mislabeled data introduced at index 22 remain in the training datasets, their negative impact on future performance is evident

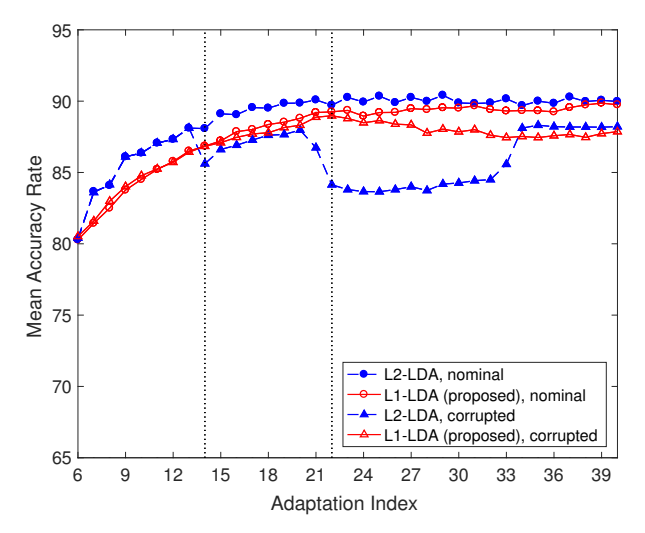


Fig. 3: Mean accuracy rate versus increment index for standard LDA and L1-LDA (proposed) under single-sample increment.

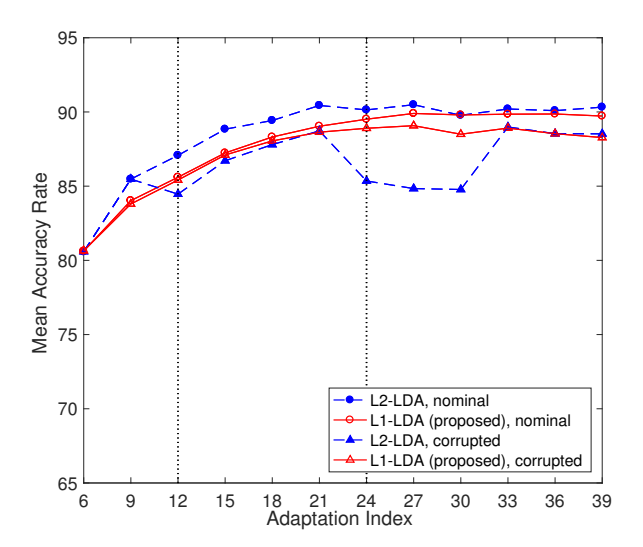


Fig. 4: Mean accuracy rate versus number increment index for standard LDA and L1-LDA (proposed) under batch-sample increment.

from the difference in mean accuracy rates under nominal and corrupted data. The results for the batch-increment case are depicted in Fig. 4, with two of the 12 new samples mislabeled and the indices where the corrupted batches are introduced indicated with a dashed vertical line. Similar observations to the single-sample increment can be made in this case as well.

IV. CONCLUSION

In this paper, we proposed an incremental version of L1norm linear discriminant analysis method for indoor human activity classification using Doppler signatures. The incremental L1-LDA permits updates of the discriminant basis as more training data become available. Due to the robustness of L1-LDA, the proposed method attains resistance to irregular corruptions of the training datasets. We validated the performance of the proposed method using real data corresponding to falling, bending, sitting, and walking. The performance of the proposed method was compared and contrasted with an incremental counterpart of standard LDA under both nominal data and outlier-corrupted data. The results demonstrated that the proposed method exhibits performance similar to that of the standard LDA for nominal training data, while it attained superior performance for corrupted data.

REFERENCES

- [1] M.G. Amin (Ed.), Radar for indoor monitoring: Detection, classification, and assessment, CRC Press, Boca Raton, FL, 2017.
- [2] F. Ahmad, A.E. Cetin, K.C. Ho, and J.E. Nelson (Eds.), "Special section on signal processing for assisted living," *IEEE Signal Process. Mag.*, vol. 33, no. 2, pp. 25-94, 2016.
- [3] F. Ahmad, R.M. Narayanan, and D. Schreurs (Eds.), "Special issue on application of radar to remote patient monitoring and eldercare," *IET Radar, Sonar, & Navig.*, vol. 9, no. 2, pp. 115-190, 2015.
- [4] M.S. Seyfioglu, A.M. Ozbayoglu and S.Z. Gurbuz, "Deep convolutional autoencoder for radar-based classification of similar aided and unaided human activities," *IEEE Trans. Aerosp. Electronic Syst.*, vol. 54, no. 4, pp. 1709–1723, 2018.
- [5] A.-K. Seifert, L. Schfer, A.M. Zoubir, and M.G. Amin, "Subspace classification of human gait using radar micro-Doppler signatures," in *Proc. European Signal Process. Conf.*, 2018.
- [6] B. Jokanovic, M. Amin, and F. Ahmad, "Radar fall motion detection using deep learning," in *Proc. IEEE Radar Conf.*, 2016, pp. 1–6.
- [7] B.Y. Su, K.C. Ho, M. Rantz, and M. Skubic, "Doppler radar fall activity detection using the Wavelet transform," *IEEE Trans. Biomedical Eng.*, vol. 62, no. 3, pp. 865–875, 2015.
- [8] M.G. Amin, F. Ahmad, Y.D. Zhang, and B. Boashash, "Human gait recognition with cane assistive device using quadratic time-frequency distributions," *IET Radar, Sonar, & Navig.*, vol. 9, no. 9, pp. 1224–1230, 2015.
- [9] S. Tomii and T. Ohtsuki, "Falling detection using multiple Doppler sensors," in *Proc. IEEE Int. Conf. e-Health Networking, Applications* and Services, 2012, pp. 196-201.
- [10] P.P. Markopoulos and F. Ahmad, "Indoor human motion classification by L1-norm subspaces of micro-Doppler signatures," in *Proc. IEEE Radar Conf.*, Seattle WA, May 2017, pp. 1807–1810.
- [11] B. Jokanovic, M. Amin, F. Ahmad, and B. Boashash, "Radar fall detection using principal component analysis," in *Proc. SPIE Defense+Security*, 2016, pp. 982919–982919.
 [12] B. Erol and M.G. Amin, "Radar data cube analysis for fall detection,"
- [12] B. Erol and M.G. Amii, "Radar data cube analysis for fall detection," in *Proc. IEEE Int. Conf. Acoustics, Speech, and Signal Process.*, 2018, pp. 2446–2450.
- [13] P.P. Markopoulos and F. Ahmad, "Robust radar-based human motion recognition with L1-norm linear discriminant analysis," in *Proc. IEEE Int. Microwave Biomed. Conf.*, 2018.
- [14] Y. Kim and T. Moon, "Human detection and activity classification based on micro-Dopplers using deep convolutional neural networks," *IEEE Geosci. Remote Sens. Lett.*, vol. 13, pp.2–8, 2016.
- [15] H. Wang, X. Lu, Z. Hu, and W. Zheng, "Fisher discriminant analysis with L1-norm," *IEEE Trans. Cybern.*, vol 44, no. 6, pp. 828–842, Jun. 2014.
- [16] F. Zhong and J. Zhang, "A Non-Greedy Algorithm for L1-Norm LDA," IEEE Trans. Image Process., vol. 26, no. 2, pp. 684–695, Feb. 2017.
- [17] V.C. Chen, D. Tahmoush, and W.J. Miceli (Eds.), Radar Micro-Doppler Signatures: Processing and applications, IET Press, London, UK, 2014.
- [18] Y. Kim and H. Ling, "Human activity classification based on micro-doppler signatures using a support vector machine," *IEEE Trans. Geosci. Remote Sens.*, vol. 47, no. 5, pp. 1328–1337, 2009.
- [19] I. Orovic, S. Stankovic, and M. G. Amin, "A new approach for classification of human gait based on time-frequency feature representations," *Signal Process.*, vol. 91, no. 6, pp. 1448–1456, 2011.
- [20] N.V. Chawla, K.W. Bowyer, L.O. Hall, and W.P. Kegelmeyer, "SMOTE: synthetic minority over-sampling technique," *J. Artif. Intell. Research*, vol. 16, pp. 321–357, 2002.